SUPPORTING INFORMATION

Mechanochemically synthesized Pb-free halide perovskite-based $Cs_2AgBiBr_6$-Cu-RGO nanocomposite for photocatalytic CO_2 reduction

Santosh Kumar,[†] Idil Hassan,[§] Miriam Regue,[†,] Soranyel Gonzalez-Carrero, [¶] Eduardo Rattner,[†] Mark A. Isaacs,[¤] and Salvador Eslava[*,†]

[†] *Department of Chemical Engineering, Imperial College London, London, SW7 2AZ, London, United Kingdom*

[§] *Department of Chemical Engineering, University of Bath, Claverton Down, Bath, BA2 7AY, United Kingdom*

[¶] *Department of Chemistry, Imperial College London, White City Campus, London W12 0BZ, UK*

[¤] *Department of Chemistry, University College London, London, WC1H 0AJ, United Kingdom*

* Corresponding author. E-mail: s.eslava@imperial.ac.uk

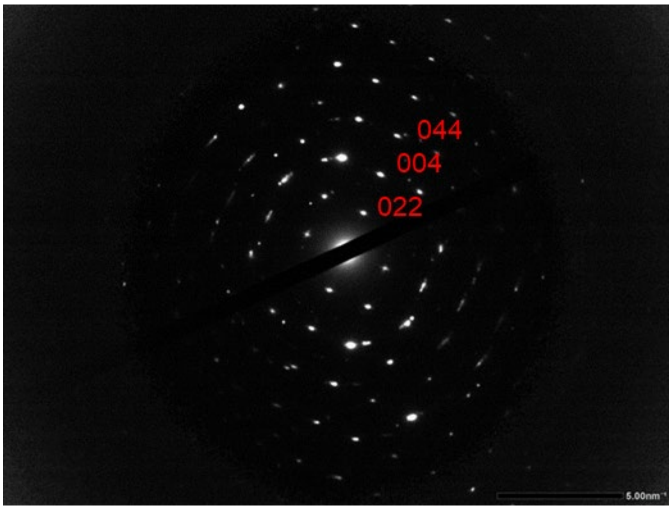

Figure S1. SAED pattern of $Cs_2AgBiBr_6$ (DP).

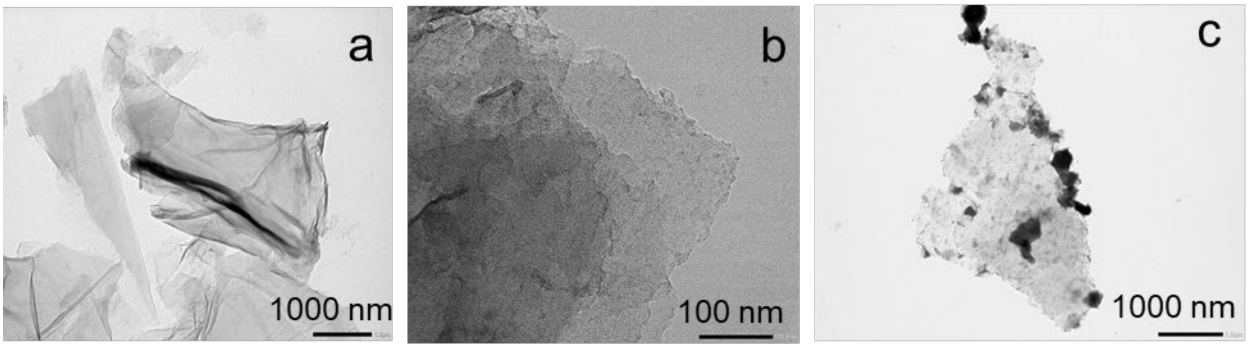

Figure S2. TEM micrographs of (a) RGO, (b) Cu-RGO and (c) DP-Cu-RGO.

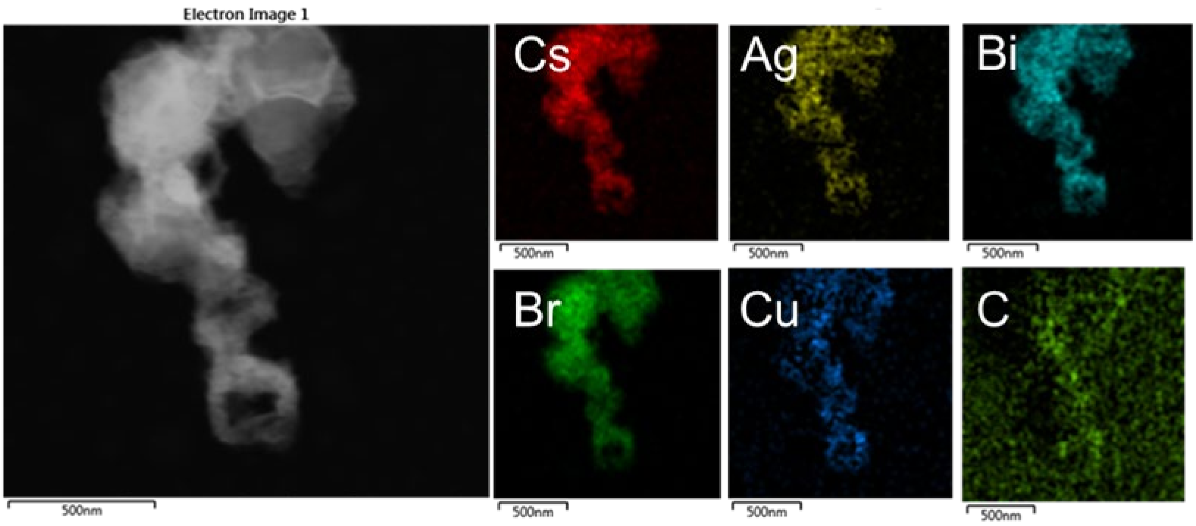

Figure S3. EDX mapping shows Cs, Ag, Bi, Br, Cu and C uniformly dispersed in the DP-Cu-RGO

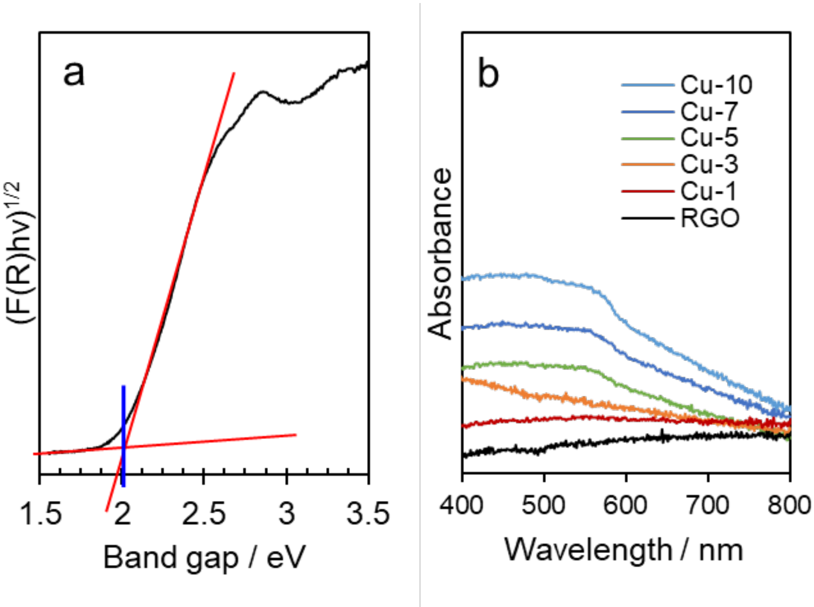

Figure S4. (a) Tauc plot to determine the optical band gap of $Cs_2AgBiBr_6$ (DP) and (b) UV-Vis DRS spectra of RGO and Cu-RGO samples with different Cu loading of 1, 3, 5, 7 and 10 wt%.

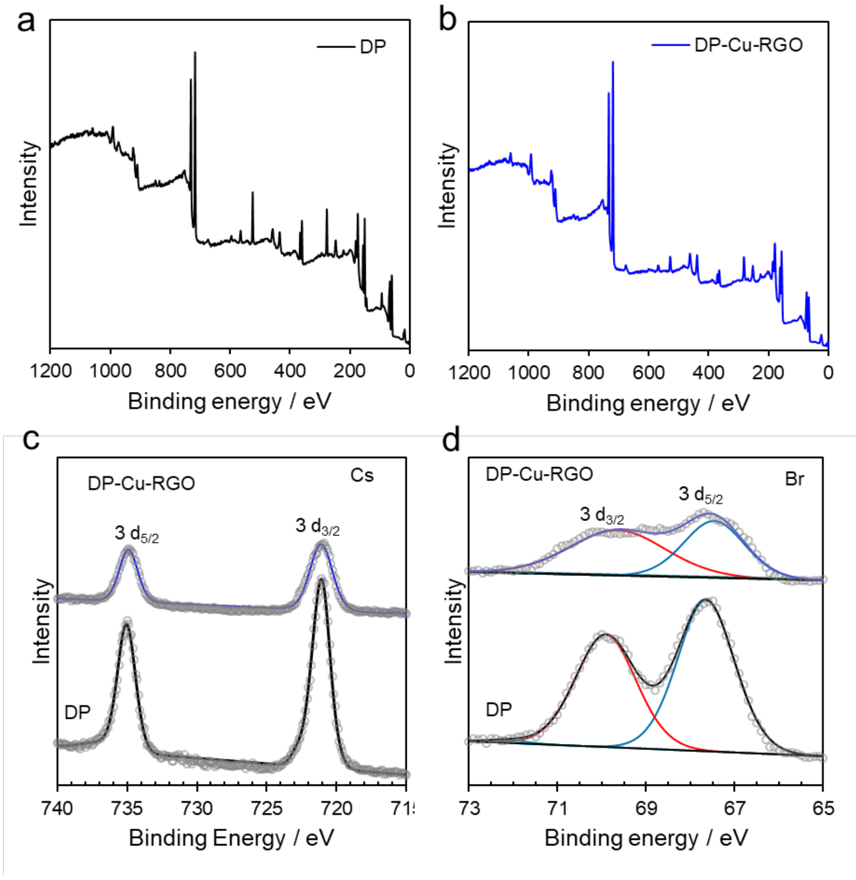

Figure S5. (a-b) Survey, (c) Cs 3d, and (d) Br 3d XPS spectra of DP and DP-Cu-RGO.

Table S1. Emission decay fitting parameters of DP and DP-Cu-RGO

	τ_1 (ns)	A_1 (%)	τ_2 (ns)	A_2 (%)	τ_3 (ns)	A_3 (%)	τ_{av} (ns)
DP	0.2	92.3	2.4	1.3	19.8	6.4	1.5
DP-Cu-RGO	0.1	99.5	0.8	0.2	12.3	0.3	0.2

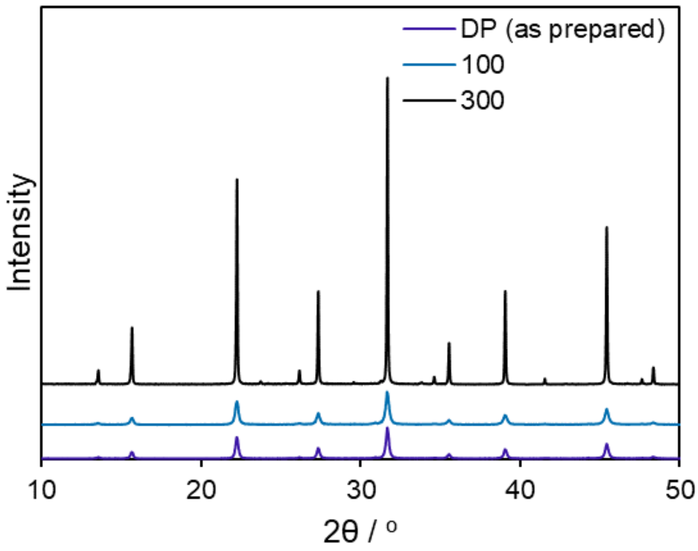

Figure S6. XRD patterns of $Cs_2AgBiBr_6$ (DP) heated at 100 and 300°C in ambient conditions.

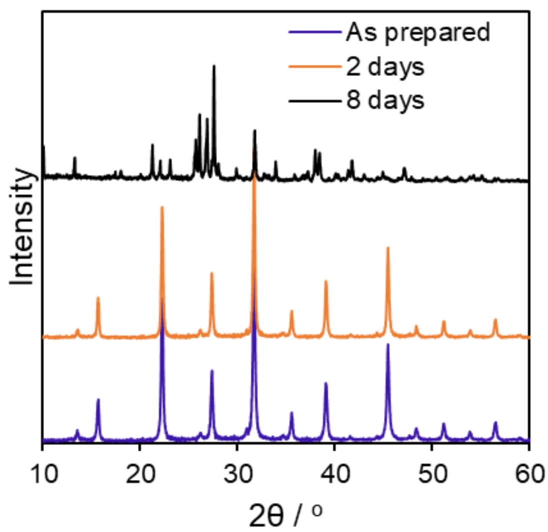

Figure S7. XRD of $Cs_2AgBiBr_6$ before and after exposing to ambient conditions (air with 60-70 % relative humidity).

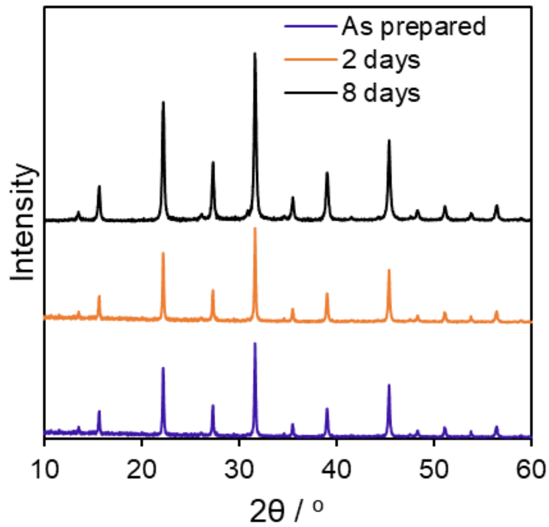

Figure S8. XRD of the as-prepared DP-Cu-RGO before and after exposing to natural environmental conditions (air with 60-70 % relative humidity).

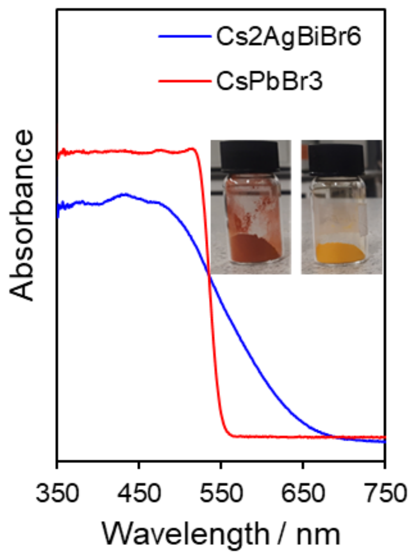

Figure S9. UV-Vis DRS spectra of $Cs_2AgBiBr_6$ and $CsPbBr_3$.

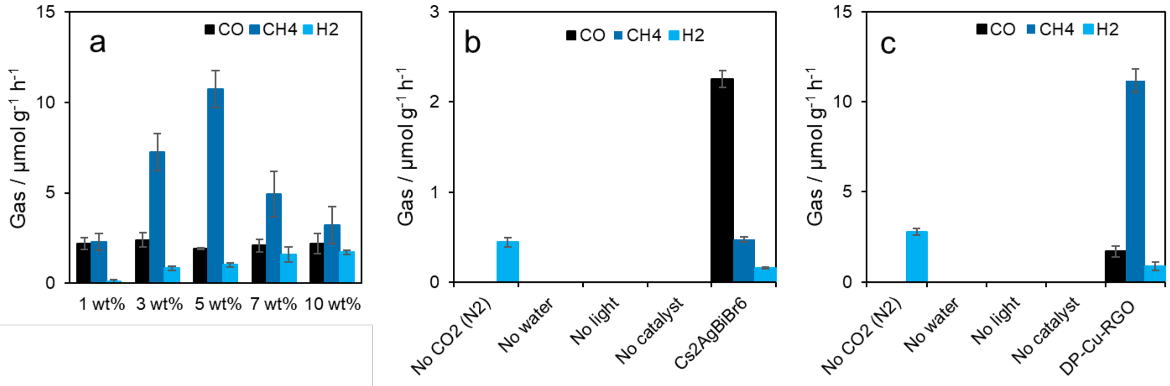

Figure S10. (a) CO, CH_4 and H_2 photocatalytic production of DP-Cu-RGO (1 wt% Cu-RGO) composites with different Cu wt% content in Cu-RGO, from 1 to 10%wt.
(b-c) CO, CH_4 and H_2 production during control experiments using (b) $Cs_2AgBiBr_6$ and (c) DP-Cu-RGO.

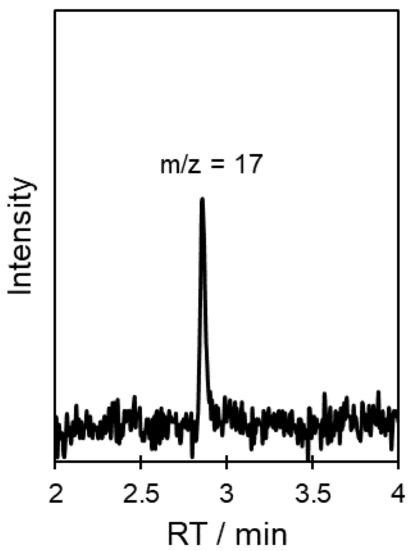

Figure S11. $^{13}CO_2$ isotope labelling experiment; m/z = 17 of $^{13}CO_2$ observed in the GCMS analysis during photocatalytic 13CO2 reduction on DP-Cu-RGO under 1 sun irradiation.

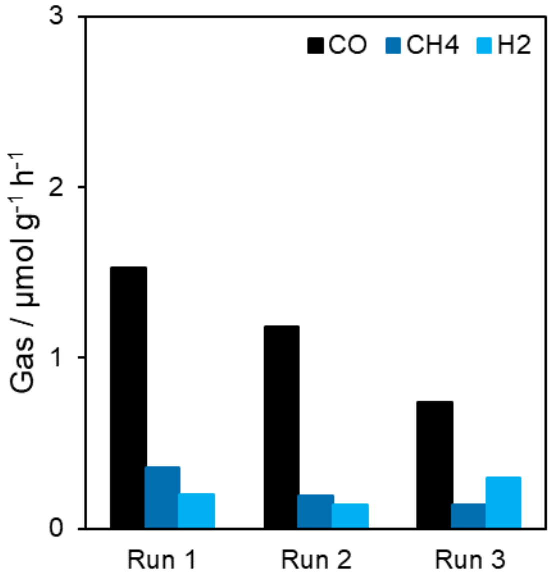

Figure S12. Reusability experiments for three successive runs of $Cs_2AgBiBr_6$. CO, CH_4 and H_2 production.

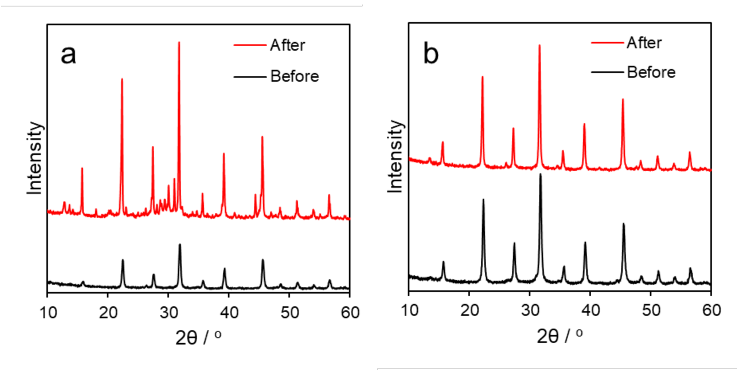

Figure 13. XRD of photocatalysts before and after 3 cycles of photocatalysis. a) DP. b) DP-Cu-RGO.

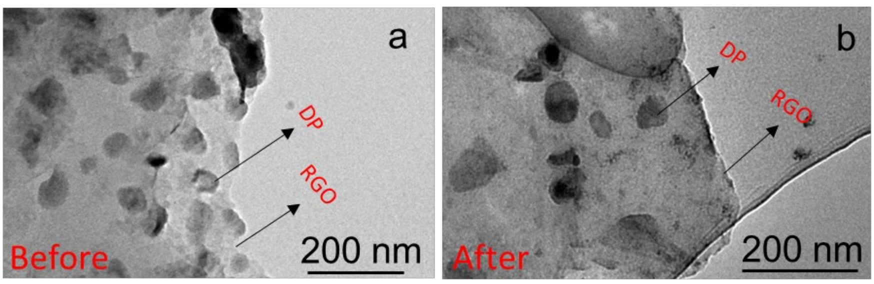

Figure S14. TEM micrographs of DP-Cu-RGO before (a) and after (b) 3 cycles of CO_2 photocatalytic reduction.

Table S2. Comparison of photocatalytic performance of DP-Cu-RGO nanocomposite for the reduction of CO_2 with various inorganic photocatalysts reported in the literature.

Material	Experimental conditions	Light source	Gas Production / µmol g^{-1} h^{-1}	AQE / %	Ref.
$ZrOCo^{II}$–IrO_x SBA-15 wafer	CO_2 and water vapor	355 nm UV light	CO (1.74)	0.001 (355 nm)	1
Cu_2O/RuO_x	1 bar CO_2 and 0.7M aqueous Na_2SO_3	150 W Xe	CO (0.32)	-	2
Cu^{II}–grafted Nb_3O_8 nanosheets	CO_2 and 0.5 M aqueous $KHCO_3$	Hg_Xe	CO (0.72)	-	3
Cu_xO–$SrTiO_3$	CO_2 and 0.5 M aqueous $KHCO_3$	Hg–Xe	CO (0.35)	-	4
Cu–PbS–QDs/TiO_2	CO_2 and water	300 W Xe	CO (0.82) CH_4 (0.58) C_2H_6 (0.31)	-	5
$In_2O_{3-x}(OH)_y$ Nanocrystals	CO_2 and water vapor	1000 W Hortilux Blue metal halide	CO (1.2)	-	6
$CuInS_2/TiO_2$	1 bar CO_2, water vapour	350 Xe Lamp	CH_4 (2.5) CH_3OH (0.86)	-	7
P25(TiO_2)–CoAl-LDH	1 bar CO_2 and water	300 W Xe	CO (2.21)	0.10 (365 nm) 0.03 (475 nm)	8
rGO/g-C_3N_4	CO_2 and water	15 W	CH_4 (14)	0.56 (420 nm)	9
Co-porphyrin/g-C_3N_4	80 kPa CO_2 TEOA and MeCN solution	300 W Xe	CO (17)	0.80 (420 nm)	10
$CsPbBr_3$ quantum dots	CO_2 and Ethyl Acetate solution	100W Xe	CO (4.3) CH_4 (1.5)	-	11
$CsPbBr_3$–GO	CO_2 and Ethyl Acetate solution	100W Xe	CO (4.8) CH_4 (2.46)	-	12
$CsPbBr_3$–ZIF-8	CO_2, water vapour	100W Xe	CH_4 (3.43)	0.035	13
$CsPbBr_3$–Porous g-C_3N_4	acetonitrile solution	300 W Xe	CO (149)	-	14
$CsPbBr_3$–Fe-basedMOFs	CO_2 and ethyl acetate or acetonitrile	300 W Xe (1 Sun)	CO (4.16) CH_4 (13.0, 66%)	-	15
$CsPbBr_3$–ZnO nanowire–macroporous RGO	CO_2, water vapour	150 W Xe	CH_4 (6.29, 96.7%)	-	16
DP–Cu–RGO	1 bar CO_2 and 60-65 % rel. humidity	300 W Xe (1 Sun)	10.7 (CH_4, 93 %)	0.89 (590 nm)	This work

References

1. W. Kim, G. Yuan, B. A. McClure and H. Frei, *Journal of the American Chemical Society*, 2014, **136**, 11034-11042.
2. E. Pastor, F. M. Pesci, A. Reynal, A. D. Handoko, M. Guo, X. An, A. J. Cowan, D. R. Klug, J. R. Durrant and J. Tang, *Physical Chemistry Chemical Physics*, 2014, **16**, 5922-5926.
3. G. Yin, M. Nishikawa, Y. Nosaka, N. Srinivasan, D. Atarashi, E. Sakai and M. Miyauchi, *ACS Nano*, 2015, **9**, 2111-2119.
4. S. Shoji, G. Yin, M. Nishikawa, D. Atarashi, E. Sakai and M. Miyauchi, *Chemical Physics Letters*, 2016, **658**, 309-314.
5. C. Wang, R. L. Thompson, P. Ohodnicki, J. Baltrus and C. Matranga, *Journal of Materials Chemistry*, 2011, **21**, 13452-13457.
6. L. He, T. E. Wood, B. Wu, Y. Dong, L. B. Hoch, L. M. Reyes, D. Wang, C. Kübel, C. Qian, J. Jia, K. Liao, P. G. O'Brien, A. Sandhel, J. Y. Y. Loh, P. Szymanski, N. P. Kherani, T. C. Sum, C. A. Mims and G. A. Ozin, *ACS Nano*, 2016, **10**, 5578-5586.
7. F. Xu, J. Zhang, B. Zhu, J. Yu and J. Xu, *Applied Catalysis B: Environmental*, 2018, **230**, 194-202.
8. S. Kumar, M. A. Isaacs, R. Trofimovaite, L. Durndell, C. M. A. Parlett, R. E. Douthwaite, B. Coulson, M. C. R. Cockett, K. Wilson and A. F. Lee, *Applied Catalysis B: Environmental*, 2017, **209**, 394-404.
9. W.-J. Ong, L.-L. Tan, S.-P. Chai, S.-T. Yong and A. R. Mohamed, *Nano Energy*, 2015, **13**, 757-770.
10. G. Zhao, H. Pang, G. Liu, P. Li, H. Liu, H. Zhang, L. Shi and J. Ye, *Applied Catalysis B: Environmental*, 2017, **200**, 141-149.
11. J. Hou, S. Cao, Y. Wu, Z. Gao, F. Liang, Y. Sun, Z. Lin and L. Sun, *Chemistry – A European Journal*, 2017, **23**, 9481-9485.
12. Y.-F. Xu, M.-Z. Yang, B.-X. Chen, X.-D. Wang, H.-Y. Chen, D.-B. Kuang and C.-Y. Su, *Journal of the American Chemical Society*, 2017, **139**, 5660-5663.
13. Z.-C. Kong, J.-F. Liao, Y.-J. Dong, Y.-F. Xu, H.-Y. Chen, D.-B. Kuang and C.-Y. Su, *ACS Energy Letters*, 2018, **3**, 2656-2662.
14. M. Ou, W. Tu, S. Yin, W. Xing, S. Wu, H. Wang, S. Wan, Q. Zhong and R. Xu, *Angewandte Chemie International Edition*, 2018, **57**, 13570-13574.
15. L.-Y. Wu, Y.-F. Mu, X.-X. Guo, W. Zhang, Z.-M. Zhang, M. Zhang and T.-B. Lu, *Angewandte Chemie International Edition*, 2019, **58**, 9491-9495.
16. Y. Jiang, J.-F. Liao, Y.-F. Xu, H.-Y. Chen, X.-D. Wang and D.-B. Kuang, *Journal of Materials Chemistry A*, 2019, **7**, 13762-13769.